



Specific features of the formation of Pt(Cu) catalysts by galvanic displacement with carbon nanowalls used as support

B.I. Podlovchenko^{a,*}, V.A. Krivchenko^b, Yu.M. Maksimov^a, T.D. Gladysheva^a, L.V. Yashina^a, S.A. Evlashin^b, A.A. Pilevsky^b

^a Department of Chemistry, Moscow State University, Moscow 119992, Leninskie Gory, Russia

^b Institute of Nuclear Physics, Moscow State University, Moscow 119991, Leninskie Gory, Russia

ARTICLE INFO

Article history:

Received 18 November 2011

Received in revised form 17 April 2012

Accepted 18 April 2012

Available online 14 May 2012

Keywords:

Carbon nanowalls (CNWs)

Copper

Platinum

Galvanic displacement

Core-shell structure

Electrocatalytic properties

ABSTRACT

Microamounts of Cu are applied by the methods of electrodeposition (Cu_{ed}) and magnetron sputtering (Cu_{spr}) on a new carbon material, carbon nanowalls (CNW). The galvanic displacement (GD) of Cu_{ed} and Cu_{spr} in a PtCl_4^{2-} solution (with 0.5 M H_2SO_4 as the supporting electrolyte) produces Pt(Cu)/CNW catalysts. The possibility of using open-circuit potential transients recorded in the course of GD for monitoring the surface layer composition is considered. The stable Pt(Cu)_{st} samples are characterized by several methods (SEM, TEM, XPS, voltammetry, etc.). It is shown that Pt(Cu)_{st} has structure of the core(Pt, Cu)–shell(Pt) type with the average atomic ratio Pt:Cu (%) \sim 57:43 for Cu_{ed} and \sim 80:20 for Cu_{spr} . The formation of the dense Pt shell is also confirmed by the data on the electrocatalytic activity of synthesized samples in the methanol oxidation reaction. The reasons for deviations in the properties of Pt(Cu)_{st}/CNW samples formed from Cu_{ed} and Cu_{spr} are discussed. The high specific surfaces of the Pt(Cu)_{st}/CNW catalyst obtained from Cu_{ed} ($>40 \text{ m}^2/\text{g Pt}$) with the simultaneous decrease in the Pt content makes this material promising for using in the platinum-catalyzed processes (particularly, in fuel cells).

© 2012 Elsevier Ltd. All rights reserved.

1. Introduction

The keen attention paid to the fuel cell problem led to the development of many methods for synthesizing nanostructured electrocatalysts based on platinum-group metals [1–3]. However, due to the high costs and the shortage of noble metals, the active quest for the ways of lowering down their content in catalysts is still continued. In doing this, the preparation of catalyst structures by means of contact displacement (replacement) of a less noble (less electropositive) metal M_1 by a noble (more electropositive) metal M_2 under the open circuit conditions seems attractive [4–14]. The method of galvanic displacement (GD) is based on the reaction: $M_1 + (n/z)M_2^{z+} \rightarrow M_1^{n+} + (n/z)M_2^0$ as a result of which metal M_1 (from submonolayer to nanosized layer) is displaced partially or completely by metal M_2 .

In electrodes of low-temperature fuel cells, the catalytic layer is often represented by Pt nanoparticles deposited on a porous carbon support. The formation of nanolayers or nanoparticles of metal M_1 on this support and their subsequent displacement by platinum (in the course of GD) allowed highly active bicomponent catalysts

with the lower platinum content to be obtained. Particularly, the core(Pt, M_1)–shell(Pt) particles were formed [7–10,13,14]. In acidic solutions, copper was used most often as metal M_1 , because the potential of the Cu/Cu²⁺ pair is sufficiently low but at the same time more positive than the potential of the standard hydrogen electrode; and, hence, the displacement of copper is uncomplicated by the parallel reaction of hydrogen evolution. The specific features of the interaction of carbon-supported copper nanolayers or nanoparticles with PtCl_6^{2-} anions were studied [8–10]. As the supports, glassy carbon (GC) [8,9] and Vulcan XC-72 soot layers applied on GC [10] were used. The gradual formation of the stable core(Pt, Cu)–shell(Pt) structures with the average Pt content of 70–75 at.% was observed. However, the electrochemically active specific surfaces of Pt(Cu) deposits were relatively small, 5–15 m²/g Pt.

It is known that the support material can substantially affect the properties of synthesized electrocatalysts (catalysts) such as the average diameter of metal particles, their size distribution, composition, stability, etc. Carbon nanotubes (CNT) are a sufficiently new electrode material [15–20] that has already found its use as the supports in the synthesis of different catalysts. However, the CNT may include traces of metals introduced by catalysts (Ni, Fe, Co, etc.) and also nanographite particles [18,20]. This makes their use difficult, especially, in the model systems employed in solving fundamental problems associated with the synthesis of

* Corresponding author. Tel.: +7 495 939 4027; fax: +7 495 932 8846.

E-mail address: podlov@elch.chem.msu.ru (B.I. Podlovchenko).

¹ ISE member.

catalysts (kinetics and mechanism of processes, structure optimization, enhancing the activity, etc.). The recently synthesized carbon nanowalls (CNW) prepared in the absence of catalysts by means of the plasma enhanced chemical vapor deposition (PECVD) [21–25] are very promising. The PECVD grown carbon nanowalls exhibited the high electric conductivity and the large specific surfaces.

In the present study, CNW were used as the supports in synthesizing the Pt(Cu)/C catalyst by the galvanic displacement of preliminarily deposited copper. Taking into account the peculiarities of the CNW structure (the presence of plate-like crystals) [21–25], it seemed interesting to elucidate how the way of copper deposition, namely, by electrodeposition as individual particles or by vacuum splaying of an even layer, affects the formation and properties of Pt(Cu) particles. Anions PtCl_4^{2-} were chosen as the displacement agent, because in their presence copper was displaced in the ratio 1:1 (for PtCl_6^{2-} : Cu:Pt = 2:1) and their reduction can proceed only to Pt (for PtCl_6^{2-} , the formation of a sufficiently stable intermediate, namely, PtCl_4^{2-} is possible).

2. Experimental

Films composed of dense array of CNW were used as the supports for platinum catalysts. CNW were grown on glassy carbon substrates in plasma of dc glow discharge in a mixture of hydrogen and methane. Details of experiments are described elsewhere [23]. The total geometric area of each GC plates was equal to 1 cm^2 .

After the synthesis of a CNW film on a GC plate, one side of the plate was covered with polystyrene, i.e., the working (accessible to polarization) surface was 0.5 cm^2 . Platinum was applied on the CNW layer by the galvanic displacement of either preliminarily electrodeposited copper (Cu_{ed}) or a copper layer sprayed on the support (Cu_{spr}) by the magnetron sputtering method. The solution containing Pt ions was $2 \times 10^{-3} \text{ M K}_2\text{PtCl}_4 + 0.5 \text{ M H}_2\text{SO}_4$. The salt K_2PtCl_4 was synthesized by the reduction of K_2PtCl_6 with hydrazine sulfate [26]. In all experiments, $0.5 \text{ M H}_2\text{SO}_4$ served as the supporting electrolyte (H_2SO_4 was of the “e.p. (Across)” grade, water was cleaned in the Milli-Q system). The measurements were carried out at $19 \pm 1^\circ\text{C}$. All potentials were related to the reversible hydrogen electrode in the same solution (RHE).

Prior to electroplating Cu or Pt, CNW were subjected to the electrochemical treatment. First of all, the electrode was polarized anodically in the $0.5 \text{ M H}_2\text{SO}_4$ supporting electrolyte solution at 1.1 V in the Ar flow for 10 min; then, after the changeover of solution, the electrode potential was brought to 0 by applying a small cathodic current. Then, the potential of 60 mV was established (the background current I_{bg} did not exceed $10 \mu\text{A}$) and the anodic I vs. E curve was measured with the potential scan rate $\nu = 6.6 \text{ mV/s}$ (the same ν was used in recording the other potentiodynamic curves). Cu electrodeposits (Cu_{ed}) were applied from the $5 \times 10^{-3} \text{ M CuSO}_4 + 0.5 \text{ M H}_2\text{SO}_4$ solution in the galvanostatic mode. The electrode potential was preliminarily stabilized in the supporting electrolyte solution at $\sim 0.4 \text{ V}$ ($I_{\text{bg}} < 5 \mu\text{A}$); then, the supporting electrolyte solution was changed in the Ar flow for a solution containing copper ions and the cathodic current of 0.2 mA was applied. The amounts of deposited copper estimated based on either the cathodic currents of Cu^{2+} deposition or the anodic currents of deposit dissolution virtually coincided ($\pm 3\%$). After the deposition of Cu_{ed} , the cell was washed with deaerated supporting electrolyte solution 7–8 times in the Ar flow while the potential was potentiostatically maintained at $E \sim 0.2 \text{ V}$. Then, the circuit was opened and the supporting electrolyte solution in the cell working part was changed for the preliminarily deaerated $0.5 \text{ M H}_2\text{SO}_4 + 2 \times 10^{-3} \text{ M H}_2\text{PtCl}_4$ solution. The time variations of the electrode potential were recorded up to the establishment of its stationary value E_{st} . Upon reaching E_{st} , the contact with the solution containing

platinum ions was broken and the cell was washed with supporting electrolyte solution in the Ar flow. The stationarity criterion corresponded to the potential variation by less than 1 mV/min . The real surface of platinum was estimated based on the desorption currents of upd copper [27–29]. As was shown in [28], for small Pt loads on the carbon support with a high intrinsic surface, the determination of the real surface of Pt based on H_{ad} becomes less reliable as compared with its determination based on Cu_{ad} . This is associated with the fact that the high intrinsic capacitance of the carbon support can substantially change with the Pt deposition, which introduces an error into the estimate of the Pt real surface. To determine the Pt surface based on Cu_{ad} , one should subtract an I vs. E curve for Pt/C (and not for C) from an I vs. E curve for $\text{Cu}_{\text{ad}}\text{Pt/C}$, i.e., the change in the capacitance of the carbon part of the surface is taken into account.

In experiments with Cu_{spr} samples, the sample was placed in deaerated supporting electrolyte solution, the electrode potential was stabilized at 0.2 V , then the circuit was opened and the chloroplatinite solution was added. The amount of Cu_{spr} was determined in a separate experiment for a sample taken from the same lot of $\text{Cu}_{\text{spr}}/\text{CNW}$ electrodes used in our experiments on the galvanic displacement of Cu_{spr} . After the stabilization of its potential at 0.2 V , an anodic potentiodynamic curve was recorded, and the amount of deposited copper was estimated from the copper desorption peak.

To obtain electrodeposited (e.d.) Pt (or Pt_{ed}) on CNW supports, the same solution $0.5 \text{ M H}_2\text{SO}_4 + 2 \times 10^{-3} \text{ M H}_2\text{PtCl}_4$ was used. After the electrode was pretreated by the same procedure as that used in electroplating of Cu on CNW, the $0.5 \text{ M H}_2\text{SO}_4$ solution was changed for the platinite solution and Pt was deposited with the cathodic current of 0.1 mA .

The electrocatalytic activity of the resulting Pt(Cu) and Pt deposits was tested in the reaction of methanol electrooxidation by measuring stationary polarization curves in the $0.5 \text{ M CH}_3\text{OH} + 0.5 \text{ M H}_2\text{SO}_4$ solution. The stationarity criterion was the current change by less than $1\%/min$ at a fixed E .

The morphology and the structural properties of samples were studied by means of scanning electron microscopy (SEM) and transmission electron microscopy (TEM). SEM images were obtained on a scanning electron microscope JEOL JSM-6490 LV with accelerating voltage of 30 kV . Transmission electron microscope JEOL JEM 2100F with accelerating voltage of 200 kV was used in order to obtain TEM images. The high resolution X-ray photoelectron spectroscopy (XPS) and the X-ray fluorescence (XRF) analysis were used for studying the chemical composition of catalysts after the deposition of platinum. XRF analysis was carried out on Inca Energy 350XT system. X-ray photoelectron spectra were recorded by a spectrometer Axis Ultra DLD (Kratos) in monochromatic $\text{Al K}\alpha$ radiation with the analyzer energy transmission of 20 eV . The analyzed region was $300 \times 700 \mu\text{m}$. The preliminary energy scale calibration corresponded to the following peaks of reference samples (ion-bombardment-cleaned metal surface): Au $4f_{5/2} - 83.96 \text{ eV}$, Cu $2p_{3/2} - 932.62 \text{ eV}$, Ag $3d_{5/2} - 368.21 \text{ eV}$, Pt $4f_{7/2} - 90.99 \text{ eV}$ with the accuracy within to $\pm 0.07 \text{ eV}$.

3. Results and discussion

3.1. Morphology of CNW and CNW-supported copper deposits

According to Fig. 1a, the original support material represents dense array of nanowalls preferentially oriented normally to towards the surface. The average height of the nanowalls is approximately $\sim 1 \mu\text{m}$ and their width is $0.5\text{--}1.0 \mu\text{m}$. TEM study (insert in Fig. 1) reveals that the average nanowall thickness is about $4\text{--}6 \text{ nm}$. According to gravimetric data, the specific mass of the CNW film is about $5 \times 10^{-6} \text{ g/cm}^2$.

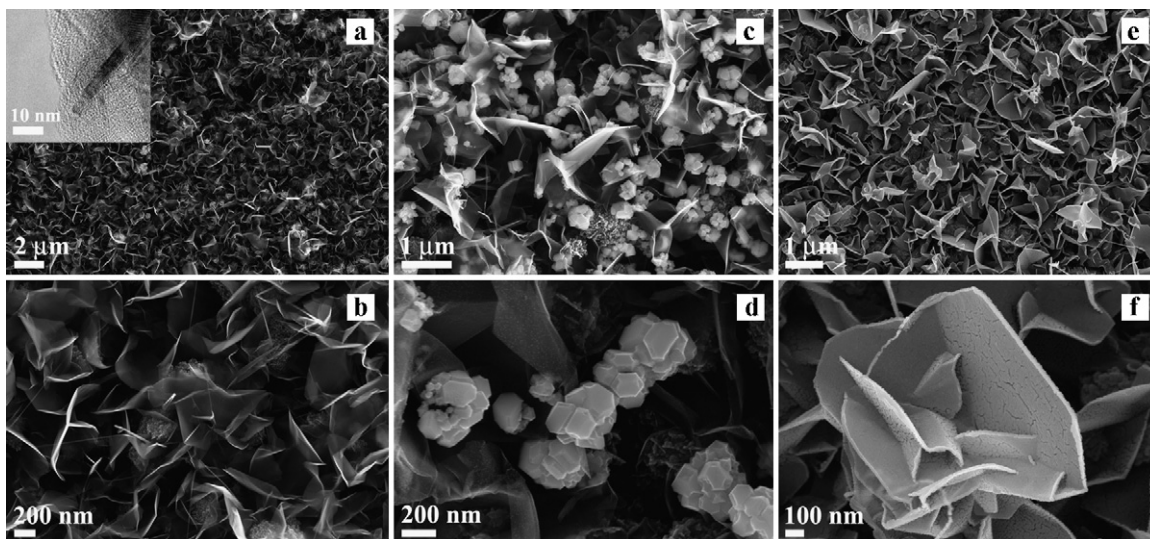


Fig. 1. SEM images of samples (a and b) as-grown CNW (inset – TEM image of the CNW); (c and d) $\text{Cu}_{\text{ed}}/\text{CNW}$ ($48 \mu\text{g}/\text{cm}^2$ geom. surf.); (e and f) $\text{Cu}_{\text{spr}}/\text{CNW}$ ($54 \mu\text{g}/\text{cm}^2$ geom. surf.).

Copper electrodeposits (e.d.) on CNW (Fig. 1c and d) represent crystals with a rather wide scatter in the size, from ~ 20 nm to ~ 200 nm. Copper was preferentially deposited on the edges of CNW and in much smaller amounts on their sides (faces); moreover, finer crystals were formed on the faces.

Fig. 1e and f shows the surface images of CNW covered with magnetron-sputtered copper. It is seen that copper is distributed evenly over both edges and faces and only strong magnification revealed the presence of cracks (< 5 nm) on certain faces.

3.2. Transients of open-circuit potential

Fig. 2 compares the open-circuit potential transients for $\text{Cu}_{\text{ed}}/\text{CNW}$ and $\text{Cu}_{\text{spr}}/\text{CNW}$ electrodes recorded upon their contact with the solution containing PtCl_4^{2-} anions (curves 1 and 2). In the first moment after the contact, a small but very quick potential surge was observed, which was associated with the sharp increase in the Cu^{2+} concentration in the near-electrode layer as the result of the reaction

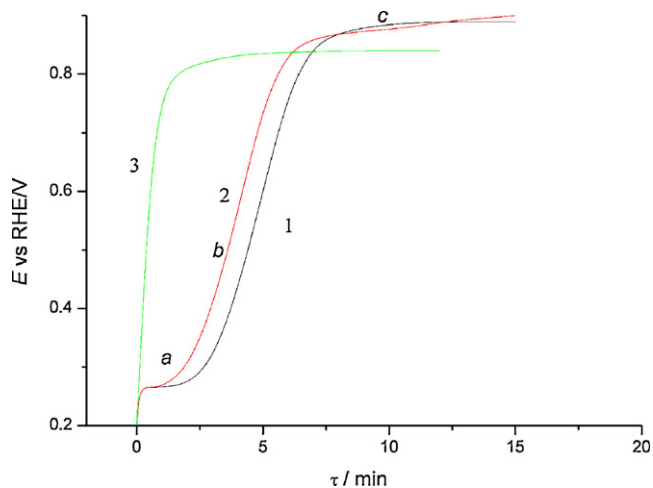
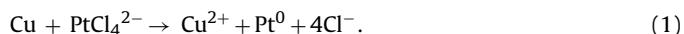


Fig. 2. Transients of open-circuit potential recorded upon bringing (1 and 2) Cu/CNW - and (3) Pt/CNW electrodes into contact with 2×10^{-3} M H_2PtCl_4 solution: (1) Cu_{ed} , (2) Cu_{spr} .

The further run of curves allows the following three segments to be singled out: a, b and c. The slow potential shift in segment a is apparently associated with the increase in the Cu^{2+} concentration with the displacement of Cu according to reaction (1), where $\text{Cu}^{2+} + 2e \leftrightarrow \text{Cu}$ remains the potential-determining stage. In segment c, the potential reaches its stationary value E_{st} (> 0.8 V) which corresponds to potentials of the beginning of oxygen adsorption on platinum. This fact alone allows one to assume the absence of considerable amounts of copper on the surface of $\text{Pt}(\text{Cu})_{\text{st}}$ particles formed at the stationary potential. At these potentials, even the copper adatoms (Cu_{ad}) most strongly bound to the surface desorbed [30,31]. The potential increase observed at $E > 0.7$ V was mainly determined by the increase in the total charge (Q [32,33]) of the platinum surface and unoccupied support areas by the reaction



Thus, after the complete displacement of Cu and Cu_{ad} ($E > 0.7$ V), under open circuit conditions, the electrons for reaction (2) are supplied by the free charge [30,31] and the partial surface oxidation of $\text{Pt}(\text{Cu})$ particles and/or support regions unoccupied by metal particles.

However, on reaching sufficiently high potential values, the oxidation of PtCl_4^{2-} to PtCl_6^{2-} starts



Assume that the stationary potential (E_{st}) of $\text{Pt}(\text{Cu})_{\text{st}}$ particles is mainly determined by the equilibrium in reaction (3). In the first approximation which ignores the activity coefficients of components of reaction (3), we can write its equilibrium potential (E_{eq}) as follows:

$$E_{\text{eq}} = E^0 + \frac{2.3RT}{2F} \log \frac{c_{\text{PtCl}_6}}{c_{\text{PtCl}_4} c_{\text{Cl}}^2} \quad (4)$$

where E^0 is the standard potential equal to 0.672 V [34]; c_{PtCl_6} , c_{PtCl_4} and c_{Cl} are the solution concentrations of PtCl_6^{2-} , PtCl_4^{2-} and Cl^- , respectively; $2.3RT/2F \approx 0.028$ V at 293 K. It is seen that E_{eq} of reaction (3) depends strongly on the concentration of chloride anions. We assume that Cl^- anions are mainly formed in reaction (1) and the degree of copper displacement is $\sim 70\%$ [8–10]. Then, for the initial copper content of ~ 0.03 mg and the cell volume of 10 ml, the chloride concentration is assessed as $c_{\text{Cl}} \approx 6 \times 10^{-4}$ M. According to Eq. (4) for $c_{\text{PtCl}_4} = 2 \times 10^{-4}$ M and $E_{\text{eq}} = E_{\text{st}} \approx 0.9$ V, we find

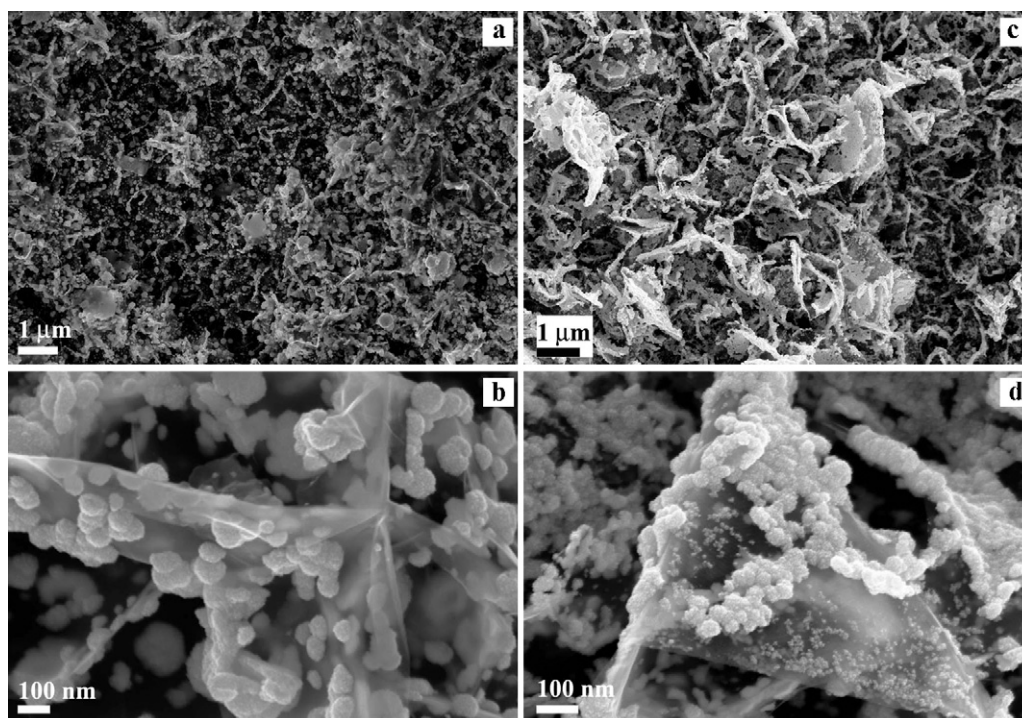


Fig. 3. SEM images of Pt(Cu)_{st}/CNW: (a and b) after the displacement of Cu_{ed} and (c and d) after the displacement of Cu_{spr}.

$C_{\text{PtCl}_6} \approx 1.4 \times 10^{-5}$ M. As seen, the oxidation of even a small part of PtCl₄²⁻ anions to PtCl₆²⁻ is in principle sufficient for potentials corresponding to the onset of oxygen adsorption on platinum (its oxidation) to be established on the Pt(Cu)/CNW electrode. Indeed, this is a rough estimate due to the very approximate nature of several assumptions made and, particularly, because the formation of Cl⁻ anions by reaction (2) was neglected. The calculations only confirmed that the role of reaction (3) in the formation of the stationary potential of Pt(Cu)_{st} particles in the presence of PtCl₄²⁻ anions may be substantial. On the whole, this is mixed a potential the establishment of which depends also on such factors as the beginning of the irreversible oxygen adsorption on Pt, the possibility of the formation of carbon oxides, the presence of microimpurities, e.g., dissolved oxygen traces that can be found even in thoroughly deaerated solutions.

Curve 3 in Fig. 2 is a transient of the open-circuit potential recorded in 0.5 M H₂SO₄ + 2 × 10⁻³ M H₂PtCl₄ solution on a CNW-supported e.d. Pt (48 μg/cm² of geometric surface) in the absence of copper on the surface. In this case, the potential increase was associated only with the increase in the total surface charge Q by to reaction (2). The gradually establishing E_{st} also lies in the potential region of the beginning of oxygen adsorption on Pt. This confirms the assumption that E_{st} on Pt(Cu)_{st} particles (curves 1 and 2) was determined by the processes that occur of the platinum surface.

The fact that E_{st} on e.d. Pt/CNW is even lower than on Pt(Cu)_{st}/CNW electrodes is rather unexpected. This is probably due to the fact that in the absence of copper in solution, the Cl⁻ anions were formed only by reaction (2). Their lower concentration in solution and, correspondingly, the lower adsorption values should favor the earlier adsorption of oxygen on platinum [32,35]. In particular, this can lead to the earlier inhibition of reaction (2) as compared with the process of formation of Pt(Cu)_{st} particles by the displacement of copper.

In segment *b* of E vs. τ curves, which corresponds to the displacement of copper (curves 1 and 2, Fig. 2), the reaction $\text{Cu}^0 \leftrightarrow \text{Cu}^{2+} + 2e$ has already stopped to be the potential-determining. Apparently,

the relatively fast potential variation in this region was mainly due to the increase in the total surface charge Q as a result of reaction (2) in the absence of considerable oxygen adsorption [32,33].

3.3. Morphology and composition of mixed Pt(Cu)_{st} deposits.

Fig. 3 shows the surface images of Pt(Cu)_{st}/CNW samples synthesized upon the displacement of either e.d. Cu (a and b) or a layer of sprayed copper (c and d). The comparison of Fig. 1(c,d) and Fig. 3(a,b) demonstrate that the metal particles are still preferentially accumulated on CNW edges but, on the whole, the number of particle increases and their size decreases. The disintegration of original Cu particles seems reasonable if for no other reason than due to the increase in the mass of metal particles, because the higher Pt atomic mass as compared with Cu is not compensated by the high specific weight of Pt (for 100% displacement of copper by platinum, the volume should increase by ~30%). Quite a lot of fine particles appear on the faces, coarser particles remain on edges. Due to the high conductivity of CNW, new particles on the faces can form due to the Pt deposition (reaction (2)) on the carbon surface areas substantially remote from the copper ionization sites ($\text{Cu} - 2e \rightarrow \text{Cu}^{2+}$). However, this does not allow us to assume *a priori* that such particles should contain no copper at all. The copper inclusion can occur due to the formation of copper adatoms (Cu_{ad}) on Pt surfaces formed at potentials <0.7 V [30,31]. This mechanism of preparation of mixed electrodeposits was considered in [36,37] for Pd–Cu and Pt–Cu deposits.

The displacement of sprayed copper produces a result at first glance unexpected. Upon reaching the stationary state in the course of displacement of copper uniformly distributed over the CNW surfaces, the Pt(Cu)_{st} deposit finds itself mostly on the CNW edges and in their vicinity (Fig. 3c and d). The metal particles on “faces” are present in insignificant amount. It is seen that the deposit represents coarse conglomerates of fine particles. The formation of such particles on CWN “faces”, which is followed by their travel to edges, appears improbable taking into account the relatively

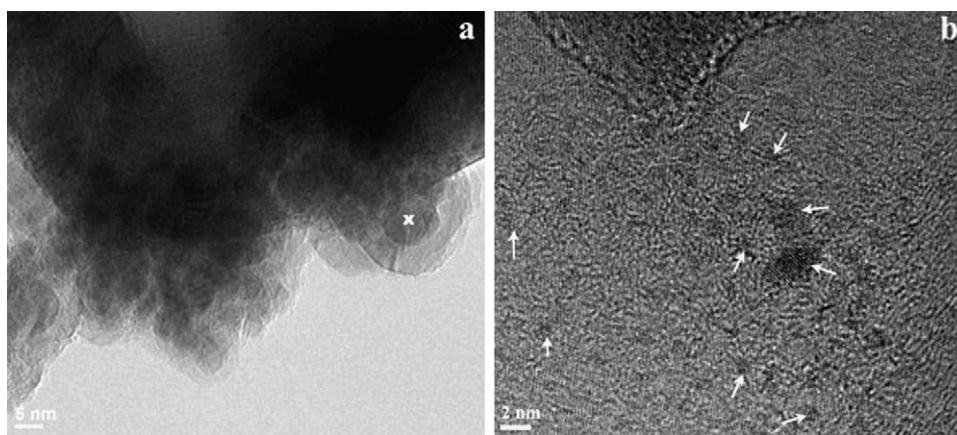


Fig. 4. TEM images of Pt(Cu)_{st}/CNW corresponding to the displacement of Cu_{ed} for (a) particles with the core-shell structure, (b) particles with the homogenous structure (some particles are marked by arrows for clarity, magnified images see in Supporting information).

short times of the mixed deposit formation. Apparently, the mechanism of spatially separated reactions $\text{PtCl}_4^{2-} + 2e \rightarrow \text{Pt}^0 + 4\text{Cl}^-$ and $\text{Cu}^0 - 2e \rightarrow \text{Cu}^{2+}$ should be preferred. It should be assumed that upon the formation of Pt(Cu) particles on edges and in their vicinity, the further deposition of Pt mainly proceeds on these particles due to the electrons donated by copper atoms from the copper layers on the faces. The uniform distribution of copper, on the one hand, provides the high total currents of its dissolution and, on the other hand, hinders the formation of Pt(Cu)_{st} particles on the faces, because this requires the destruction of the copper layer. Although in the proposed mechanism of sprayed copper displacement the incorporation of copper into the platinum deposit through copper adatoms is, as was noted above, possible, one, however, should expect the lower copper content as compared with the formation of Pt(Cu)_{st} particles from e.d. Cu on CNW. Indeed, this assumption confirms the results of the XRF analysis of the average contents of Pt and Cu in Pt(Cu)_{st}/CNW deposits shown in Table 1 (the total content of Pt and Cu atoms was assumed to be 100%). Among the other factors that can explain the preferential deposition of Pt on CNW edges at the Cu_{spr} displacement, mention should be made of the different electric field gradients on the edges and side walls of CNW and also of the difference in the discharge kinetics of PtCl₄²⁻ anions on Pt and Cu.

It is interesting that Pt(Cu)_{st} particles synthesized by the GD method from e.d. Cu on CNW contained a noticeably larger amount of copper as compared with the case where GC [8,9] and carbon black [10] were used as the support. The reason for this may consist in the accumulation of the main mass of the original copper deposit on CNW edges. The displacement of copper in the upper layers of such deposit and the agglomeration of Pt(Cu) particles formed strongly hinder the dissolution of copper located in the bulk of coarse conglomerates. This assumption is also confirmed by the results on the dissolution of Pt–Cu alloys in sulfuric acid solution saturated with air [38]. The sharp inhibition of copper dissolution

observed in 5–10 min after the beginning of the corrosion process was associated [38] with the formation of a dense platinum layer.

The TEM examination of Cu_{ed}/CNW and Pt(Cu)_{st}/CNW (from Cu_{ed}) samples was carried out. On the whole, these images confirmed the SEM data (Figs. 1d and 3b). For Cu_{ed}/CNW, no new information was obtained (these TEM images are omitted). Fig. 4 shows the TEM images for Pt(Cu)_{st}/CNW, which are the most interesting from our point of view. Fig. 4a demonstrates a particle (marked with a cross) with the core-shell structure (the core with the diameter of ~10 nm and the shell with the thickness of ~5 nm). A conglomerate of such particles can be seen to the left of the former particle.

Fig. 4b demonstrates TEM image of CNW decorated with particles with the linear size of 1–4 nm. These particles have a homogeneous bulk structure with the interplanar spacing of about 0.21 nm. This is close to the interplanar spacing for Pt *hkl* (1 1 1) and (2 0 0). Based on the XPS and electrochemical data (see below) it can be concluded that these are Pt particles. Thus, the TEM data show that Pt(Cu)_{st} particles prepared by the GD method differ not only in the size but also in the composition. In this connection, it can be said that the application of the term “core-shell” to Pt(Cu)_{st}/C systems prepared by galvanic displacement is to a certain extent conditional.

The specific surfaces of Pt(Cu)_{st}/CNW (from Cu_{ed}) samples related to 1 g Pt in the deposit were 46(±15) m²/g, whereas for the directly deposited Pt, the surface was 2–3 times smaller (see Table 1). Earlier, the much lower *S* values were obtained for the galvanic displacement of Cu_{ed} from GC [8,9] and Vulcan XC-72 soot [10] (see Section 1). Apparently, this is associated with the higher dispersivity of Cu_{ed} on CNW. In line with this, the displacement of Cu_{spr} led to the formation of Pt(Cu)_{st} with the lower specific surfaces (Table 1).

3.4. The composition of the surface layer of Pt(Cu)_{st} particles (XPS analysis)

The XPS results point to the formation of a continuous surface layer of metal platinum with the thickness of 2–3 nm (the atomic ratio Cu/Pt ≈ 1/99). Analytical Cu 2*p* peak on the general X-ray photoelectron spectrum (not shown) is virtually absent. Fig. 5 demonstrates Cu 2*p* and Pt 4*f*s spectra. The continuity of surface layer was attested by the fact that copper was detected in its unoxidized state. The Cu 2*p* peak is described by a single doublet with the binding energy BE(Cu 2*p*_{3/2}) = 931.76 eV. The formation of core-shell structures can be concluded based on the comparison of atomic

Table 1

Characteristics of Pt(Cu)_{st}/CNW electrodes: *m*_{Cu}, the original mass of Cu; Pt:Cu, the composition of the Pt(Cu)_{st} deposit; *m*_{Pt}, the amount of Pt in Pt(Cu)_{st} deposit; *S*, specific surface.

| <i>m</i> _{Cu} (μg) (deposit type) | Pt:Cu (at.%) | <i>m</i> _{Pt} (μg) | <i>S</i> _{Pt} (m ² /g) |
|--|--------------|-----------------------------|--|
| 24.5 (e.d.) | 56:44 | 43.3 | 61.2 |
| 24.3 (e.d.) | 54:46 | 39.0 | 45.6 |
| 24.0 (e.d.) | 60:40 | 44.2 | 31.0 |
| 14.0 (spr) | 82:18 | 43.0 | 17.1 |
| 27.6 (spr) | 78:22 | 66.1 | 10.9 |
| Pt (e.d. without Cu) | | 40.0 | 20.1 |

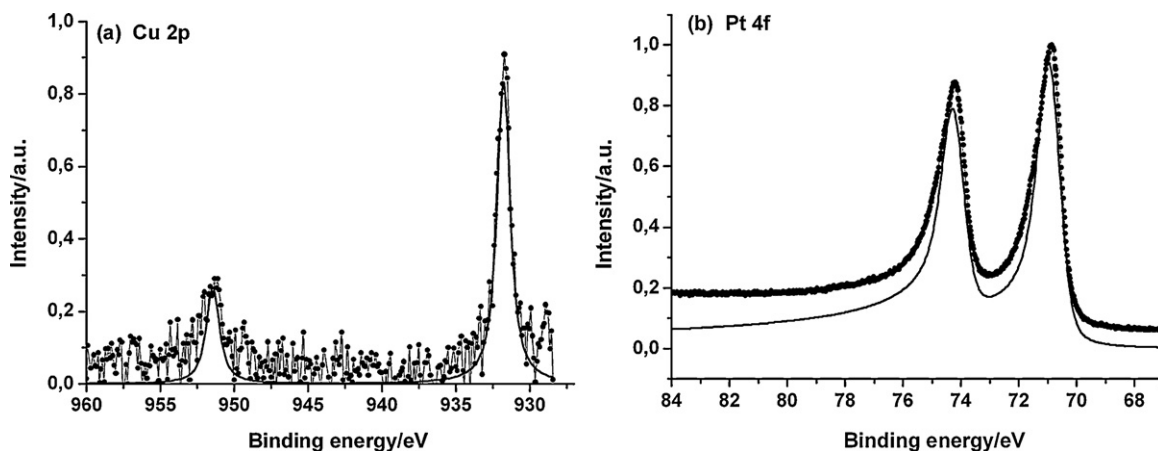


Fig. 5. X-ray photoelectron spectra of Pt(Cu)_{st}/CNW: (a) Cu 2p; (b) Pt 4f. Points – data obtained experimentally, line – fitting with the Gaussian/Lorentzian convolution.

ratios of metals found by a volume method (XPF) and a method for analyzing the surface (XPS). These results suggest that platinum is largely accumulated in the surface layer.

It should be noted that the Cu 2p_{3/2} peak is shifted by ca. 1 eV to the lower binding energies, which is considerably lower as compared with elemental copper. This may indicate that the latter is accumulated in the “core” in its intermetallic state.

The analysis of Pt 4f spectrum revealed that the found parameters are completely identical to those obtained for pure platinum foil; the peak corresponds to the energy of 70.9 eV and is characterized by the asymmetry parameter $\alpha = 0.22$, i.e., pertains to the volume state. It is well known from the literature [39,40] that the decrease in the size of platinum clusters from 5 to 1 nm can shift the Pt 4f_{7/2} peak to the higher binding energies by ~ 1 eV and decreases asymmetry. The absence of these effects suggests that in the material under study, platinum particles with sizes fitting this range are preferentially in the electric contact with one another; hence, one can speak of their “conglomeration”.

3.5. Voltammetric characteristics of Pt(Cu)_{st}/CNW electrodes.

Fig. 6 shows that the potentiodynamic curves of Pt(Cu)_{st}/CNW electrodes obtained by the galvanic displacement of either e.d. Cu (curve 2) or sprayed Cu (curve 3) are very close to the similar curve for e.d. Pt on CNW (curve 1). Both curves demonstrate well pronounced hydrogen regions; their double-layer regions contain no peaks or waves of ionization of bulk and/or upd copper. Thus, the electrochemical results together with the XPS data point to the formation of the shell(Pt)–core(Pt, Cu) structures and the virtually total absence of copper in the surface layer of particles.

The anodic potentiodynamic curves of the desorption of the monolayer of copper adatoms from two types of Pt(Cu)_{st}/CNW electrodes and also from the Pt_{ed}/CNW electrode are also sufficiently close (Fig. 7).

To assess the degree of permeability of the Pt shell for copper atoms in the core, we considered the peculiarities of the behavior of copper adatoms on a Pt electrode. As it was shown in [28,30], the Cu_{ad} monolayer (Cu_{ad} ML) accumulated the e.d. Pt remains on the surface even after the repeated washings of both the electrode and the cell working part with the thoroughly deaerated supporting electrolyte (sulfuric acid) solution. Hence, were the shell permeable, the stabilization the Pt(Cu)_{st}/CNW electrode at the potential of the formation of Cu_{ad} ML would result in the exit of copper to the surface in the form of adatoms. The anodic potentiodynamic curve of the Pt(Cu)_{st}/CNW electrode (with originally e.d. copper) measured after the exposure of the electrode to 0.5 M H₂SO₄ at $E = 300$ mV for 3 h (insert in Fig. 6) demonstrated the appearance of

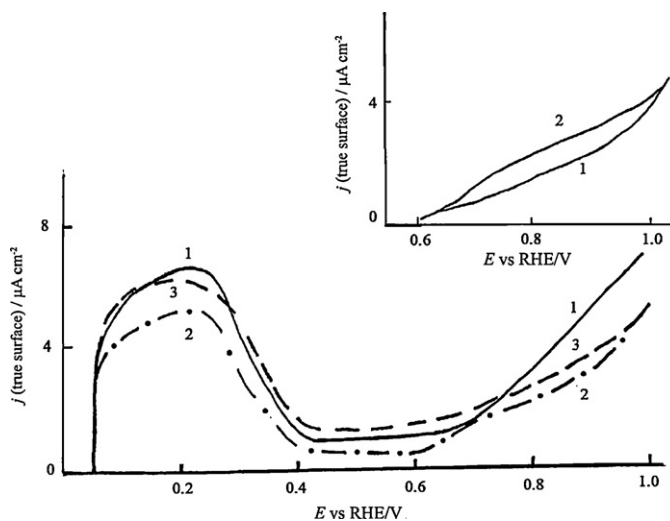


Fig. 6. Anodic potentiodynamic curves of (1) Pt_{ed}/CNW and (2 and 3) Pt(Cu)_{st}/CNW electrodes: (1) e.d. Pt (80 μg/cm² of geometric surface); (2 and 3) prepared from: (2) Cu_{ed} (48 μg/cm² of geometric surface), (3) Cu_{spr} (54 μg/cm² of geometric surface). Supporting electrolyte 0.5 M H₂SO₄. Insert: parts of anodic potentiodynamic curves for Pt(Cu)_{st}/CNW (from Cu_{ed}): (1) background, (2) after the electrode exposure to 0.5 M H₂SO₄ solution at 0.3 V for 3 h (see explanations in the text).

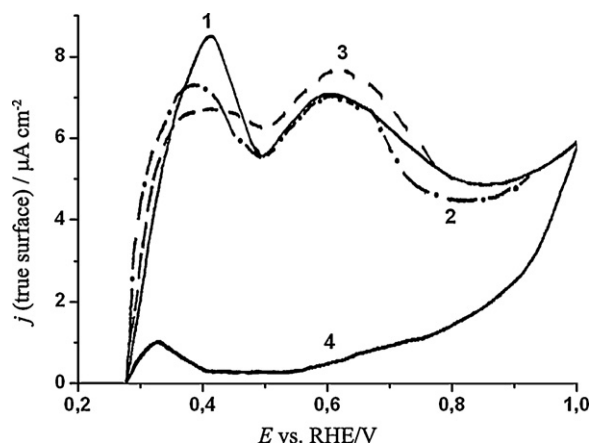


Fig. 7. Anodic potentiodynamic curves for Pt_{ed}/CNW (1 and 4) and Pt(Cu)_{st}/CNW (2 and 3) in the presence (1–3) and in the absence (4) of Cu_{ad} on the surface: (2) Cu_{ed}, (3) Cu_{spr}.

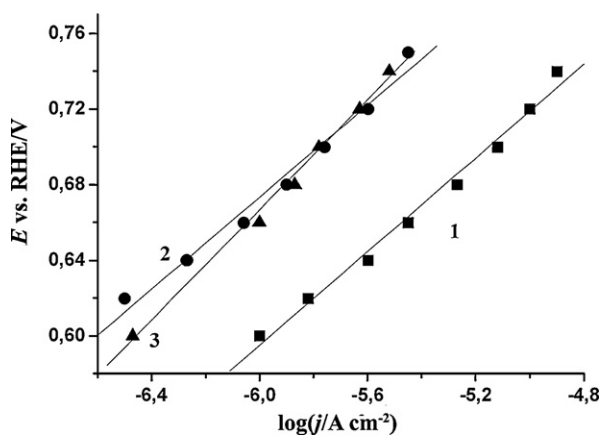


Fig. 8. Steady-state polarization curves of methanol electrooxidation (0.5 M $\text{CH}_3\text{OH} + 0.5 \text{ M H}_2\text{SO}_4$) on (1) $\text{Pt}_{\text{ed}}/\text{CNW}$ and (2 and 3) $\text{Pt}(\text{Cu})_{\text{st}}/\text{CNW}$: (2) Cu_{ed} , (3) Cu_{spr} . Specific current densities (j) are given per cm^2 of the true surface.

a small wave at the potentials of ionization of copper adatoms. As regards the charge consumed in the ionization of Cu_{ad} , the average rate of copper exit was assessed as $\sim 2 \text{ nA}/\text{cm}^2$ of the real surface area. Indeed, such a slow rate of the copper exit cannot have any noticeable effect on the cyclic voltammograms even recorded with the slow potential scan rate used here.

A certain difference in the adsorption of oxygen is observed in the initial region of the oxygen potential range for three electrodes under consideration (Fig. 6). This can be associated with the different sizes and different distributions of catalyst particles over the carbon support surface. In these potential regions, the CNW surface can also be somewhat oxidized, which is initiated by the presence of catalytically active Pt particles. It is seen that the oxide (this can also be OH species) formation [41,42] on $\text{Pt}_{\text{ed}}/\text{CNW}$ electrodes in 0.5 M H_2SO_4 occurs a little earlier (at less positive potentials) as compared with the $\text{Pt}(\text{Cu})_{\text{st}}/\text{CNW}$ electrodes. This agrees with the assumption that the difference in E_{st} for $\text{Pt}(\text{Cu})_{\text{st}}$ and Pt particles on CNW (Fig. 2) can be due to the difference in the oxygen adsorption at least in the range of low surface coverages.

3.6. Electrooxidation of methanol on $\text{Pt}(\text{Cu})_{\text{st}}/\text{CNW}$ electrodes

According to result shown in Fig. 8, the specific rates of methanol electrooxidation (calculated per cm^2 of the electrode surface determined based on the upd copper desorption) on the $\text{Pt}(\text{Cu})_{\text{st}}/\text{CNW}$ electrodes prepared by the displacement of Cu_{ed} and Cu_{spr} , are close to one another. They do not exceed (and are even somewhat lower) the specific rate of CH_3OH oxidation on the $\text{Pt}_{\text{ed}}/\text{CNW}$ electrode with the close amounts of deposited Pt. This agrees with the

conclusion [10] that the presence of copper in the cores of $\text{Pt}(\text{Cu})_{\text{st}}$ particles has no activating effect on the stationary process of CH_3OH electrooxidation.

From our point of view, the results of polarization measurements in CH_3OH solutions agree with the other results of the present study and confirm the presence of a sufficiently dense Pt layer on the surface of $\text{Pt}(\text{Cu})_{\text{st}}$ particles. The fact that the CH_3OH electrooxidation currents on the $\text{Pt}(\text{Cu})_{\text{st}}$ deposit proved to be somewhat lower than on e.d. Pt are best explained by the structural factors, particularly, the size effect. For Pt particles incorporated into polymer matrices, the “negative” size effect (a decrease in the process rate on small particles) was observed [43] in the reaction of methanol oxidation. The comparison of SEM images of $\text{Pt}(\text{Cu})_{\text{st}}/\text{CNW}$ (Fig. 3) and $\text{Pt}_{\text{ed}}/\text{CNW}$ (Fig. 9) surfaces made it possible to conclude that Pt electroplates contained virtually no crystals measuring less than 10 nm, whereas $\text{Pt}(\text{Cu})_{\text{st}}$ deposits contained a lot of such particles. According to SEM and TEM data (Figs. 3 and 4), the sizes of certain $\text{Pt}(\text{Cu})_{\text{st}}$ particles synthesized of GD did not exceed 2–3 nm. The increase in activity of Pt particles in the reaction of methanol oxidation (MOR) as their size increased from ~ 2.5 to $\sim 6.5 \text{ nm}$ was mentioned in [44]. The same paper cites many studies in which the “negative” size effect was also observed for MOR on platinum catalysts. Usually, two main factor that determine this effect are distinguished [43,44]: (i) the large particles are more “convenient” for multisite adsorption of the CH_3OH molecule, (ii) on small Pt particles, the O and/or OH adsorption is stronger, which inhibits their interaction with methanol chemisorptions products. However, the different MOR rates on $\text{Pt}(\text{Cu})_{\text{st}}/\text{C}$ and $\text{Pt}_{\text{ed}}/\text{C}$ can be associated, as well, with factors other than the size effect, for instance, the specifics of the methanol/ CO_2 transport on the “stuck together” agglomerates of $\text{Pt}(\text{Cu})_{\text{st}}$ particles and/or the changes in the ratio of stable products of CH_3OH oxidation (CO_2 , HCOOH , H_2CO).

The strong difference in the morphology of e.d. Cu (Fig. 1c and d) and e.d. Pt (Fig. 9) was quite unexpected. Obviously, in contrast to Cu, platinum is sufficiently uniformly distributed over the CNW surface without any preferential deposition on the edges and demonstrates no substantial scatter in the particle size for the average size of $\sim 35 \text{ nm}$. The calculation of the specific surface according to the model of spheres gave $\sim 8 \text{ m}^2/\text{g}$. This is approximately 2 times lower than S of Pt_{ed} on CNW, determined based on upd copper desorption, although at the high magnification, one can see that sphere-like particles with the mentioned average sizes represent conglomerates formed by bounded together crystals with linear size of several nm. Thus, there is a considerable differences in the surface structures of $\text{Pt}(\text{Cu})_{\text{st}}$ particles and e.d. Pt particles formed on CNW.

The problem of the reason for such a different distribution of Cu and Pt electroplates on CNW is very interesting on its own right but

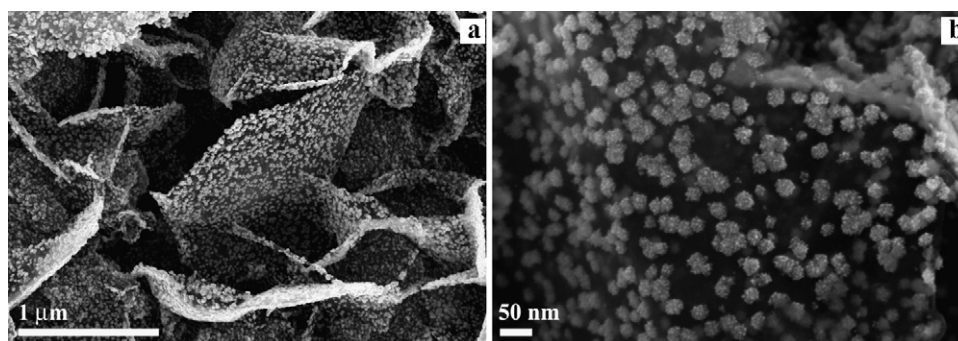


Fig. 9. SEM images of e.d. Pt ($80 \text{ g}/\text{cm}^2$ geom. surf.) on CNWs.

goes beyond the frames of the present study. It can also be mentioned that the strong difference in the charge and the structure of Cu^{2+} and PtCl_4^{2-} ions allows one to expect a substantial difference between their discharge mechanisms and, hence, between the nucleation sites for Pt and Cu crystals.

4. Conclusions

It was shown that CNW can be successfully used as the supports in the preparation of Pt(Cu) catalysts by the method of galvanic displacement.

- The possibility of using transients of open-circuit potential for monitoring the surface layer composition in the course of GD in systems in which the displaced non-noble metal represents a phase deposit is analyzed.
- It was found that the Pt(Cu)_{st}/CNW system, which exhibits the properties of stable structures of the shell(Pt)–core(Pt, Cu) type, really represents a mixture of particles differing in not only their size but also the composition.
- The specific activity of Pt(Cu)_{st} electrodes in the reaction of methanol oxidation (calculated per cm² of the real surface) turned out to be some lower than the activity of the Pt_{ed}/CNW electrodes, which was explained by the size effect.
- A comparison of characteristics of Pt(Cu)_{st}/CNW synthesized from Cu_{ed} and Cu_{spr} allowed us to reveal the important role played by the spatially separated reactions of Cu dissolution and Pt deposition in the GD.
- The Pt(Cu)_{st}/CNW catalyst synthesized based on Cu_{ed} exhibited the high specific surface and the smallest content of Pt as compared with analogous catalysts described in the literature. This might be of certain interest for practice.

Acknowledgment

The work was financially supported by the Russian Foundation for Fundamental Research, Project Nos. 12-03-00998a and MK-4994.2012.2.

Appendix A. Supplementary data

Supplementary data associated with this article can be found, in the online version, at <http://dx.doi.org/10.1016/j.electacta.2012.04.124>.

References

- [1] T.R. Ralph, M.P. Hogarth, *Platinum Metals Review* 46 (3) (2002) 117.
- [2] W. Vielstich, A. Lamm, H. Gasteiger (Eds.), *Handbook of Fuel Cells, Fundamentals, Technology, Applications* (Hardcover), J. Willy and Sons, London, 2003.

- [3] C. Conntanceau, S. Brimand, C. Lamy, J.-M. Leger, L. Dubau, S. Rousseau, F. Vigier, *Electrochimica Acta* 53 (2008) 6865.
- [4] S.R. Brankovic, J.X. Wang, R.R. Adzic, *Surface Science* 477 (2001) L173.
- [5] M.B. Vukmirovic, J. Zhang, K. Sasaki, A.U. Nilekar, F. Uribe, M. Mavrikakis, R.R. Adzic, *Electrochimica Acta* 52 (2007) 2257.
- [6] Y. Yu, Y. Hu, X. Liu, W. Deng, X. Wang, *Electrochimica Acta* 54 (2009) 3092.
- [7] M. Van Brussel, G. Kokkinidis, I. Vandendael, C. Buess-Herman, *Electrochemistry Communications* 4 (2002) 808.
- [8] S. Papadimitriou, A. Tegou, E. Pavlidou, S. Armanyanov, E. Valova, G. Kokkinidis, S. Sotiropoulos, *Electrochimica Acta* 53 (2008) 6559.
- [9] S. Papadimitriou, S. Armanyanov, E. Valova, A. Hubin, O. Steenhaut, E. Pavlidou, G. Kokkinidis, S. Sotiropoulos, *Journal of Physical Chemistry C* 114 (2010) 5217.
- [10] B.I. Podlovchenko, T.D. Gladysheva, A.Yu. Filatov, L.V. Yashina, *Russian Journal of Electrochemistry* 46 (2010) 1189.
- [11] D. Gokcen, S.-E. Bae, S.R. Brankovic, *Electrochimica Acta* 56 (2011) 5545.
- [12] D.-Y. Park, H.S. Jung, Y. Rheem, C.M. Hangarter, Y.-I. Lee, J.M. Ko, Y.-H. Choa, N.V. Myung, *Journal of Physical Chemistry C* 114 (2010) 5217.
- [13] N. Kristian, Y. Yu, J.-M. Lee, X. Liu, X. Wang, *Electrochimica Acta* 56 (2010) 1000.
- [14] P. Wang, H. Li, H. Feng, H. Wang, L. Lei, *Journal of Power Sources* 195 (2010) 1099.
- [15] W. Gang, X. Bo-Qing, *Journal of Power Sources* 174 (2007) 148.
- [16] J. Prabhuram, T.S. Zhao, Z.H. Liang, R. Chen, *Electrochimica Acta* 52 (2007) 2649.
- [17] Z. Liu, X.Y. Ling, L. Hong, J.Y. Lee, *Journal of Power Sources* 167 (2007) 272.
- [18] J. Li, Y. Liang, G. Bing, X. Zhu, X. Tian, *Electrochimica Acta* 54 (2010) 1277.
- [19] A.A. Mikhaylova, E.K. Tusseeva, N.A. Mayorova, A.Yu. Rychagov, Yu.M. Volkovich, A.V. Krestinin, O.A. Khazova, *Electrochimica Acta* 56 (2011) 3656.
- [20] C.L. Scott, M. Pumera, *Electrochemistry Communications* 13 (2011) 426.
- [21] Y. Ando, X. Zhao, M. Ohkohchi, *Carbon* 35 (1997) 153.
- [22] Y.H. Wu, P.W. Qiao, T.C. Chong, Z.X. Shen, *Advanced Materials* 14 (2002) 64.
- [23] V.A. Krivchenko, V.V. Dvorkin, N.N. Dzbanovsky, M.A. Timofeyev, A.S. Stepanov, A.T. Rakhimov, N.V. Suetin, O.Yu. Vilkov, L.V. Yashina, *Carbon* 50 (2012) 1477.
- [24] M. Hiramatsu, M. Hori, *Carbon Nanowalls: Synthesis and Emerging Applications*, Springer, NY, 2010.
- [25] B. Zheng, Y. Kehan, L. Ganhua, W. Pengxiang, M. Shun, Ch. Junhong, *Carbon* 49 (2011) 1858.
- [26] N.N. Chernyaev (Ed.), *Synthesis of Complex Compounds of Platinum Group Metals*, Nauka, Moscow, 1964.
- [27] T.D. Gladysheva, B.I. Podlovchenko, Z.A. Zikrina, *Electrochimica Acta* 23 (1987) 1440.
- [28] T.D. Gladysheva, B.I. Podlovchenko, *Vestnik Moskovskogo Universiteta Seriya 2 Khimiya* 38 (1997) 3.
- [29] C.L. Green, A. Kucernak, *Journal of Physical Chemistry B* 106 (2002) 1036.
- [30] T.D. Gladysheva, B.I. Podlovchenko, *Electrochimica Acta* 35 (1999) 573.
- [31] B.I. Podlovchenko, U.E. Zhumaev, Yu.M. Maksimov, *Journal of Electroanalytical Chemistry* 651 (2011) 30.
- [32] A.N. Frumkin, *Potentsialy Nulevogo Zaryada (Zero-Charge Potentials)*, Nauka, Moscow, 1981.
- [33] B.I. Podlovchenko, E.A. Kolyadko, *Journal of Electroanalytical Chemistry* 506 (2001) 11.
- [34] A.J. Bard, F. Sholz, M. Stratmann, Ch.J. Pickett (Eds.), *Encyclopedia of Electrochemistry, Inorganic Chemistry*, vol. 7, Textbooks-Barnes and Noble/Wiley-VCH, 2007, p. 43.
- [35] N. Li, J. Lipkowski, *Journal of Electroanalytical Chemistry* 491 (2000) 95.
- [36] B.I. Podlovchenko, Ju.M. Maksimov, T.L. Azarchenko, E.N. Egorova, *Electrochimica Acta* 30 (1994) 258.
- [37] D.-L. Lu, M. Ishihara, K. Tanaka, *Electrochimica Acta* 43 (1998) 2325.
- [38] Y. Hosh, T. Yoshida, A. Nishikata, T. Tsuru, *Electrochimica Acta* 56 (2011) 5302.
- [39] J.H. Tian, F.B. Wang, Zh.Q. Shan, R.J. Wang, J.Y. Zhang, *Journal of Applied Electrochemistry* 34 (2004) 461.
- [40] T. You, O. Niva, M. Tomita, S. Hirono, *Analytical Chemistry* 75 (2003) 2008.
- [41] B.E. Conway, *Progress in Surface Science* 49 (1995) 331.
- [42] G. Yerkiewicz, G. Vatankhah, J. Lessard, M.P. Soriaga, Y.-S. Park, *Electrochimica Acta* 49 (2004) 1451.
- [43] Yu.M. Maksimov, B.I. Podlovchenko, T.L. Azarchenko, *Electrochimica Acta* 43 (1998) 1053.
- [44] S.H. Joo, K. Kwon, D.J. You, Ch. Pak, H. Chang, J.M. Kim, *Electrochimica Acta* 54 (2009) 5746.